

Experimental and numerical analysis of heat transfer from main vessel to safety vessel using H_2O/Al_2O_3 nanofluid in a nuclear reactor vault

M. Anish^{a,*}, B. Kanimozhi^b, N. Beemkumar^b, Jayaprapakar J.^b

^aDepartment of Mechanical Engineering, Sathyabama Institute of Science and Technology, Chennai, India, email: anish2010me@gmail.com

^bSchool of Mechanical Engineering, Sathyabama Institute of Science and Technology, Chennai, India, emails: kanitohre@yahoo.com (B. Kanimozhi), beem4u@gamil.com (N. Beemkumar), jp21tn@gmail.com (Jayaprapakar J.)

Received 10 October 2017; Accepted 13 April 2018

ABSTRACT

Nuclear reactor produces electricity by fission reaction of uranium and neutron. Due to this reaction, a lot of heat energy is produced. Hence, this must be kept under control or else the components of reactor core may get damaged which in turn leads to radiation leakage which affect the surrounding environment. Ever since nuclear plants came into operation, dissipation of heat is done by water. But some inert gases that have good heat transfer coefficient and good thermal conductivity for heat dissipation process. The ultimate aim of this project is to find out how efficiently a nanofluid and argon gas can dissipate heat from the reactor vault as a coolant in a circuit. The most commonly used nanofluid is Al_2O_3 nanoparticle with water or ethylene as base fluid. Al_2O_3 has good thermal properties and it is easily available. In addition, it can be stabilized at various pH levels. The various temperature distribution leads to different characteristic curves and the characteristic curves give detailed report to enhance heat transfer rate from main vessel to safety vessel. The nanofluid used for the heat transfer process is a combination of Al_2O_3 (nanoparticle) and therminol 55 (base fluid). The alumina nanoparticle is mixed with therminol 55 at 0.01 vol% concentration. Formerly, the experiments have been conducted by using water and nitrogen gas this leads to poor heat transfer rate. We alternatively conducted this experiment by using nanofluid and argon gas for nurturing the heat transfer rate.

Keywords: Al_2O_3 nanoparticles; Convective radiation; Heat dissipation; Therminol; Nuclear reactor; Inert gases; Nanofluids; Sonification; Reactive plates

1. Introduction

Commercial fast breeder reactor (CFBR) is a 500 MWe sodium cooled pool type reactor. It has three main heat transport circuits, that is, primary sodium, secondary sodium and steam water system. The heat generates in the reactor core is removed by the circulating primary sodium passing through the core subassemblies from bottom to top. The primary sodium transfers heat to the secondary sodium through intermediate heat exchangers. The secondary sodium heats up water in the steam generators to raise steam for running turbine to produce electric power. All reactor internals including core and primary sodium circuit are contained in a

single vessel called main vessel [19]. The top shield forms the top cover for the main vessel, and it consists of roof slab, large rotatable plug, small rotatable plug and control plug. The top shield provides thermal and biological shielding from the hot sodium pool to facilitate the personnel access [1]. This study intends to spotlight the flow boiling heat transfer attainment of metal oxide and multi-walled carbon nanofluids innermost part of an annulus heat exchanger. In the meanwhile, pool boiling of the mixtures of citric acid/water on a horizontal heated cylinder and the nucleate pool boiling heat transfer coefficients were measured [2]. This study gives how the boiling mechanism is entrenched on a copper made heater at different concentration of nanofluid. Results demonstrated that heat transfer coefficient of titana nanofluids are nearly higher than that of the base fluid. Heat and mass concentration of nanoparticles can reinforce the pool boiling heat

* Corresponding author.

transfer coefficient, while subcooling temperature can only have crunch on formation of bubbles [3]. To enhance the pool boiling heat transfer coefficient of pure liquid, based on the gas injection through the liquids has been introduced. Hence, the ramification of gas dissolved in a stagnant liquid on pool boiling heat transfer coefficient has experimentally been investigated [4]. The nanoparticles issue on water heat transfer demonstrated that the presence of nanoparticles into liquid phase due to surpassing their thermal conductivity results in intensifying the heat transfer mechanism [5].

Based on the experience gained during design, manufacture and erection of components of prototype fast breeder reactor, many innovative features are considered for the components of the reactor assembly of CFBR. It enhances the safety and improved economy. Nanofluids were primed by using two-step method at weight concentration of 0.1%–0.4%. Role of sonification time and the stability were discussed [6]. The higher thermal performance was carried out in CuO/water nanofluid comparison with water, which has lower pressure drop and pumping power against the gallium. Results also divulge that CPU is cooled more readily with gallium at overload and normal working modes [7]. Investigating on the operating parameters illustrated that with increasing the heat flux and flow rate of nanofluid, heat transfer coefficient of nanofluid dramatically increases [8]. In contrast, with increasing the volumetric concentration of nanofluid, controversial condition is observed such that increases the heat transfer coefficient in forced convective region is reported, while reduction of heat transfer coefficient is seen for nucleate boiling zone [9]. In this context, it is proposed to reduce the thickness of the safety vessel from 20 to 6 mm. To facilitate this, the gap between safety vessel and reactor vault need to be reduced. So movements under seismic events will be directly transmitted to the vault. The reduction in gap also results in reduction of overall diameter of the reactor. However, due to reduced gap between vault and safety vessel, the vault liner needs to be integrated with safety vessel along with the insulation panels. This is to avoid difficulties during erection of entire safety vessel along with the insulation panels into reactor vault through narrow gap. The constructability of this arrangement needs to be demonstrated [10]. Furthermore, the reduced gap may lead to increase the heat load to the concrete. Prior to undertaking, the demonstration and constructability are the integrated system and experimental validation of thermal design, it has been proposed to conduct heat transfer studies on a reactor vault of size 1 m × 1 m × 1,800 mm with integrated safety vessel. To simulate this heat transfer to safety vessel, a heater plate simulating main vessel along with embedded heaters was fabricated and erected with a gap of 250 mm and the reactor vault temperature was maintained by cooling fluid circulation system [11].

2. Methodology

The aim of this project is to study the experimental and numerical analysis of heat transfer from main vessel to safety vessel by using nanofluid and argon gas. The operation dissipation of heat is done by water in the nuclear plants. Apart from this, there are a lot of gases which have heat transfer coefficient and good thermal conductivity. The ultimate aim

of this project is to find out how efficiently nanofluids and argon gas can dissipate heat from the reactor vault circuit. Presently, the nuclear plants are using water to carry out the heat energy from reactor vault. It has certain limitations of boiling point, scale forming, pH value and poor heat caring capacity. Modern technology gives an alternate solution by using nanofluid instead of water. Nanofluid has higher rate of heat transfer property than water [12]. Applying various temperature limits to main vessel leads to various temperature curves and the temperature distribution up to the end of concrete wall.

3. Preparation of nanoheat transfer fluid

The preparation methodology and the characterization of alumina (Al_2O_3)-therminol 55 are shown in Fig. 1. Spherical Al_2O_3 nanoparticle with 99.5% purity refractive index with 1.768 and surface area with 32–40 m^2/g are used to prepare nanoheat transfer fluid [13]. The nanoparticle used in this process has an average size of 30–40 nm [14]. Therminol 55 is used as a base fluid since it has good miscibility and viscosity. However, to further minimize the potential for fluid oxidation, system utilizing heat transfer fluids should be blanketed with an inert atmosphere [15]. Therminol 55 is noncorrosive to metals commonly used in the design of heat transfer systems. The recommended optimum economic bulk temperature (550°F/290°C) is based on detailed thermal studies. Operation at this temperature provides long service life under most operating conditions. Therminol 55 can be utilized up to the maximum temperature of 315°C. Volatile products should be vented from the system to a nonhazardous area away from personnel and sources of ignition. The high-boiling compounds are generally soluble in the fluid [16]. Overheating will accelerate this decomposition and may result in separation of the high-boiling compounds as solids (tar, coke, etc.). These solids could be detrimental to the operation of the system and, when detected, should be removed.

Figs. 1 and 2 show the magnetic stirrer that is used to disperse nanoparticle into base fluid. The stability of the nanofluid is necessary in order to maintain the stability of the



Fig. 1. The magnetic stirrer.

nanofluid. Or else nanofluid can lose their potential to transfer heat. The stability method used in this process is ultrasonic bath. Then the mixture is kept in the ultrasonic bath for 30 to 40 min in order to improve the stability of the nanofluid and this process is known as sonification. This process is used to prepare nanofluid of Al_2O_3 -therminol 55 combination with a volumetric concentration of 0.05%. Furthermore, this process is used to prepare nanofluid of various volumetric concentrations such as Al_2O_3 , 0.025, 0.05, 0.075, 0.1, 0.2 and 0.3 vol%.

Therminol 55 can be used as a base fluid as it has good miscibility and viscosity. The amount of nanoparticles is to be added to achieve a concentration of 0.05 (Fig. 3).

An amount of 0.48 g Al_2O_3 nanoparticle is measured using electronic weighing machine and is dispersed in 1 L of therminol 55 base fluid. Then the mixture is kept in magnetic stirrer and is left for around 15–25 min. Therefore, allowing the nanoparticle is completely dispersed into the base fluid.

Argon was initially discovered by English scientists when they realized that there was something other than nitrogen, oxygen, carbon dioxide and water in the air. Lord Rayleigh and Sir William Ramsay were finally able to isolate this mysterious substance in 1894, discovering the first noble gas which they named “argon” (Greek for “lazy” or “slow”) in reference to its inactivity. Argon is nontoxic, non-reactive and has a thermal conductivity approximately 30% lower than air [17]. On the periodic table, argon falls into the class of noble gasses including helium, neon, krypton and xenon. However, they are more expensive than argon [18]. It is a naturally occurring gas that makes up 0.934% of the

earth’s atmosphere by volume. It is heavier than air with a density of 1.784 g/L compared with the density of air of 1.29 g/L. It is not flammable and will not burn or explode as a gas. It is colorless, odorless and tasteless, and since it occurs naturally in the atmosphere. It is not a threat to the environment. No threshold limit value, permissible exposure limit or maximum acceptable level has been established for normal exposure to the gas. It is also noncorrosive. In order to avoid the heat conduction to the stainless steel (SS) sheets of the thermal insulation from the studs welded to the safety vessel, a ceramic sleeve is provided around the studs. The stud holes in the SS sheets are oblong shaped in order to accommodate the thermal expansion between the stud fixing points. In that experimental setup, the green highlighted position is the insulation system. It is used to reduce the heat transfer into the concrete reactor from the safety vessel. A system has to be designed to ensure minimal heat transfer outside from the safety vessel which could be reliable in the long run, since maintenance and repairs are hardly possible. As specified, the heat generated value is pretty high so that it needs the thermal insulation.

5. Design model of the proposed setup

The experimental setup was first designed in solid works with accurate and precise dimensions as shown in Fig. 4 [19–24]. In this figure, only three reflective plates are shown to give a better understanding on how the plates are introduced into the system. All the 34 plates are arranged in the similar manner. As shown in the above figure, reflective plates of dimension 1,000 mm × 1,000 mm × 0.1 mm are attached to the mild steel (MS) plate and it is insulated or covered by the use of ceramic wool of thickness 30 mm. The insulating material is used in the ceramic wool due to its excellent insulating properties and it can withstand high temperature (up to 1,200°C). The ceramic wool of dimension 600 mm × 7,000 mm × 30 mm is used in order to form the casing of the setup. The casing is made out of insulating material in order to make sure that heat flow takes place only through the SS plates and not through casing. A plate heater of dimension 1,000 mm × 1,000 mm × 250 mm is used in the setup to supply required heat. The power rating of the heater is 230 V and 8 A. It is capable of generating temperature as high as 600°C and the base material is used as MS. Two MS plates of dimension 1,000 mm × 30 mm × 30 mm are used to form the casing and also to attach the plate heater to the setup.



Fig. 2. Ultrasonic bath.

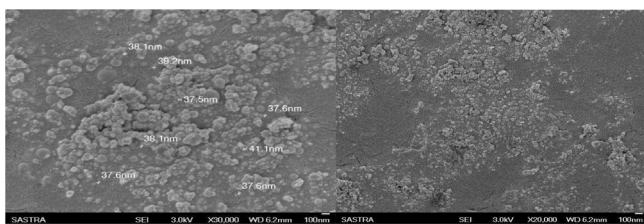


Fig. 3. SEM images at 20,000× and 30,000× magnification of Al_2O_3 nanoparticles.

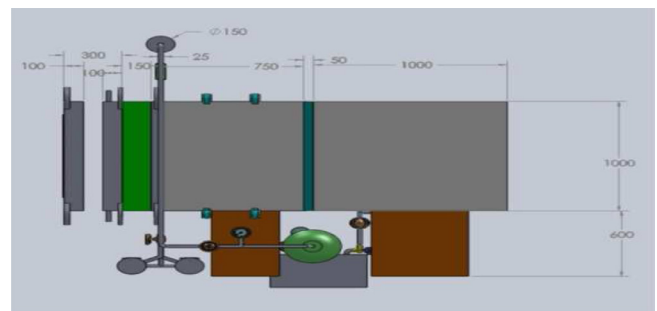


Fig. 4. Design of total assembly setup.

6. Design of total assembly setup

The safety vessel consists of 34 no. of 0.1 mm thickness reflective plates stacked parallel leaving uniform gap between them. The SS plates are bound together by using panel which is made up of SS material. The plates attached to the MS plate by the use of rods which is covered with SS plates welded to the MS plates.

After attaching the SS plates on the MS plates, it is fixed in the rods and these plates are insulated by the use of insulation material which is made up of ceramic wool. The insulation material (ceramic wool) can withstand the temperature up to 1,200°C (Fig. 4). The 34 SS plate dimensions are 1 m × 1 m and a gap of 150 mm is maintained between the MS plates. A gap of 4.5 mm is maintained between the each SS plates, so that heat transfer due to conduction process will be avoided. These parallel plates are acted as insulation by reflecting radioactive heat emanating from the safety vessel thereby it restricts the heat flow in the reactor vault. Therefore, radiation and conduction are the modes of heat transfer through the insulation panel. Radioactive heat transfer is a function of surface emissivity of the insulation plates. Emissivity of polished SS plates is varied slightly with temperature. However, this variation of emissivity value is not taken into account. For numerical and theoretical calculation purpose, the emissivity value of reflective SS plate is conservatively taken as 0.05. Since the plates are very thin (0.1 mm). The thermocouples are attached to the plates by the use of laser welding process to avoid blackening and also to avoid the damage in the SS plates. The thermocouples are attached only to the plain SS sheets. The scope of this project is limited to one-dimensional heat flow. This is the main reason for fabricating the external casing with an insulating material. And then the MS and SS plates are kept just before the liner plate made up of MS material.

7. Fabrication of the experimental setup

The experimental setup is fabricated in accordance with the design which is shown in Figs. 6, 7, 9 and 10. The plates are attached on opposite sides of the casing to act as inlet and outlet. Plate heater is attached to the inlet MS plate to act as a heat source, a thermocouple is also attached along with it to measure the heater temperature. In order to prevent heat loss, the entire experiment is sealed effectively by using a ceramic wool. It is fabricated in such a way that there is only one-dimensional heat flow inside the setup. Inside, the setup consists of nitrogen gas. Thermocouples are attached on each plate with the help of a nut. The nuts are welded to each plate with the help of arc welding. Thermocouples are laser welded to the SS insulation sheets by laser welding technique so that the properties of the sheets are not affected. The other end of the thermocouples (which has to be connected to the indicator) is drawn out of the setup by making holes on the ceramic wool material and then sealing it efficiently to eliminate the heat loss. The plates are inserted into the guide bar by means of collars attached to the plates. To avoid twisting while inserting the plate on the rod, the rod is fully embedded in the concrete. The insulation material used in the setup should resist temperatures up to 600°C. Therefore, ceramic wool was used as an insulation material. The ceramic wool

available in wide varieties of thickness and have countless applications. The density of the ceramic wool is 64 kg/mm³. A roll of ceramic wool was purchased. And the dimensions of ceramic wool material are 600 mm × 7,000 mm × 30 mm (Fig. 5).

8. Liner plate, cooling circuit and concrete

The liner plate is made up of MS plate of dimensions of 1,100 mm × 1,100 mm × 6 mm. Five numbers of square section cooling pipes of dimension 25 mm × 25 mm × 3 mm are welded to the liner plate at a pitch of 200 mm. The square pipes are connected to three headers, top header and two bottom headers. The outlet of the top header is connected to the heat exchanger inlet and the outlet of heat exchanger is connected to water tank. A 0.5 HP pump is provided in the tank to circulate water through the circuit. Two square pipes are connected to the bottom left side header and three square pipes are connected to the bottom right side header. The bottom headers receive water from the tank with the



Fig. 5. Fabrication of experimental setup.

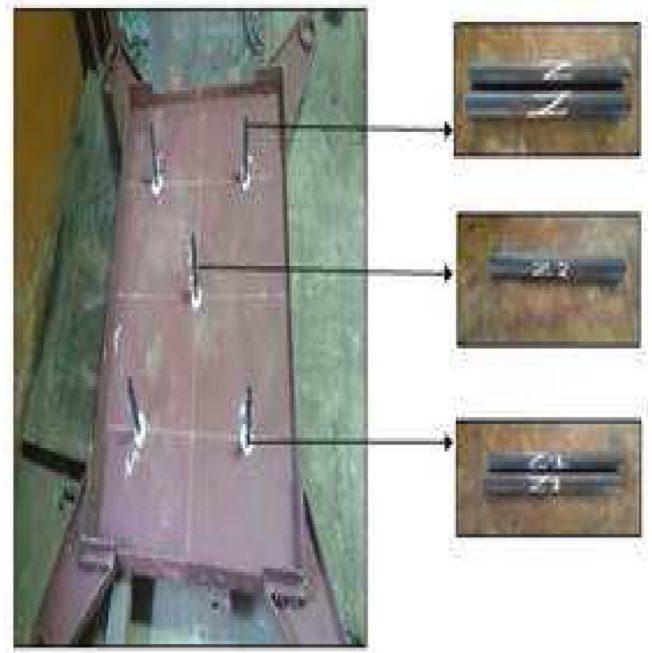


Fig. 6. Studs welded to safety vessel plate.

help of a pump. Each inlet pipe is provided with pressure gauge and control valve to regulate the flow of water through the circuit. A bypass valve is also provided at the pump outlet to control the flow of water through the circuit. The flow meters are provided in the square pipes to measure the water flow rate. The water when passes through the square pipes welded to the liner plate it gets heat and the hot water is sent to top header. From this header, the water flows through the heat exchanger where it is cooled and supplied to the tank. The water from the tank is recirculated through the circuit by means of a pump. The two layers of concrete reactor vault (750 mm and 1,000 mm) are separated by 50 mm thick expanded polystyrene (EPS) insulation. The concrete vault is fabricated in accordance with the design. The reactor vault setup is constructed with M-30 concrete in rectangular shape of 1,800 × 1,100 × 1,100 mm (Fig. 8).

9. Experimental work

An experimental program has been undertaken in the model to study the temperature distribution at various

locations in the main vessel, safety vessel, thermal insulation, liner, cooling pipes and concrete. The experiments have been conducted to maintain the main vessel at different temperature level of 100°C, 200°C, 300°C, 400°C, 500°C and 577°C with all the five cooling pipes working. The cooling fluid flow rate through the pipes welded to liner plate is maintained at 6 lpm. The temperature at 64 locations in the model has been noted down at steady-state condition. The temperature distribution graphs are plotted with respect to sensor locations. The setup is numerically analyzed by using ANSYS R15.0. Finally, the results have been compared with the experimental results. Experimental uncertainty analysis is an approach that analyses a derived quantity, based on the uncertainties in the experimentally measured quantities that are used in some form of mathematical relationship (“model”) to calculate the derived quantity. Uncertainty analysis is often called the “propagation of error.” In addition, to measure the uncertainty of each run of experiment, mathematical mean square method has been employed. In this research, ΔT equals to ± 0.2 according to accuracy of each thermocouple and Δq equals to 0.25%.



Fig. 7. Heater embedded with ceramic tiles.

10. Results and discussion

In this trial, the temperature of main vessel (heater plate) is set at different temperature level of 100°C, 200°C, 300°C, 400°C, 500°C and 577°C; and the temperature at various locations of the model are noted at steady-state condition. Figs. 11–16 show the temperature of safety vessel – MS plate temperature, insulation panel temperature, liner temperature and concrete vault temperature.

11. Numerical analysis

Numerical analysis of the model is done by using ANSYS R15.0. The steps followed in the analysis are as follows:

11.1. The property module

The properties of the materials for the different parts of the model are assigned by using PROPERTY module. The properties are assigned in Table 1.

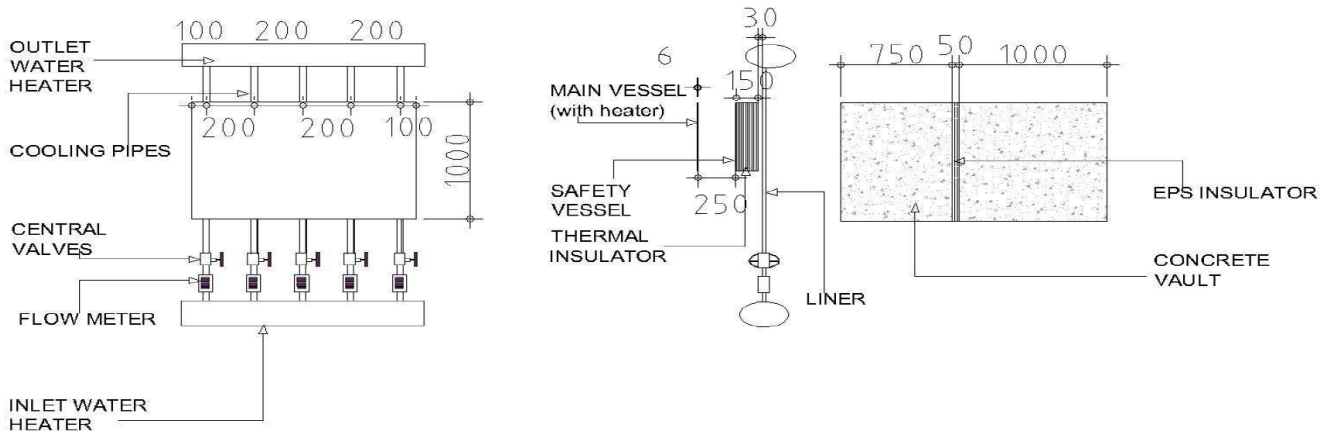


Fig. 8. Cooling circuit and concrete structure.



Fig. 9. k-Type thermocouple (wire type).



Fig. 10. k-Type thermocouple (steel type).

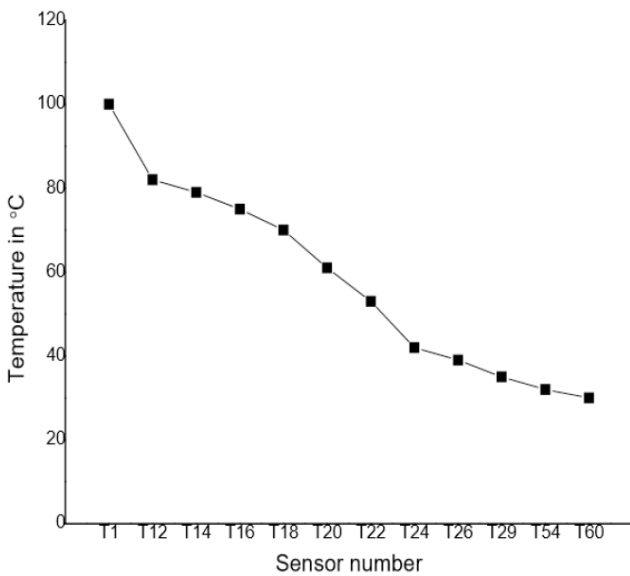


Fig. 11. Temperature distribution when main vessel is set at 100°C.

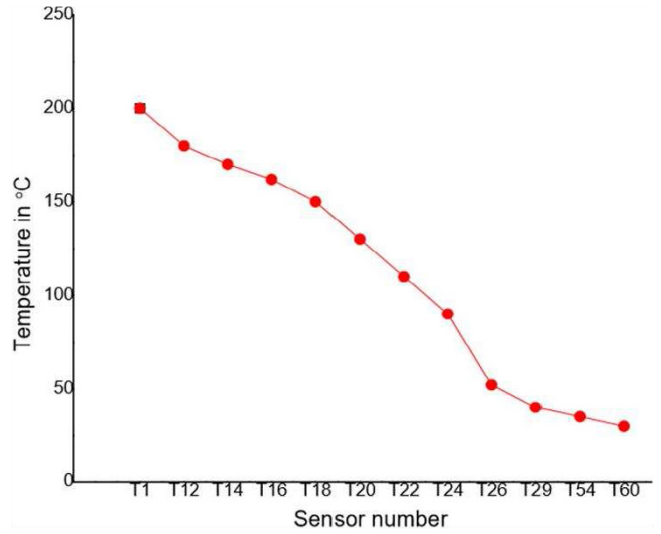


Fig. 12. Temperature distribution when main vessel is set at 200°C.

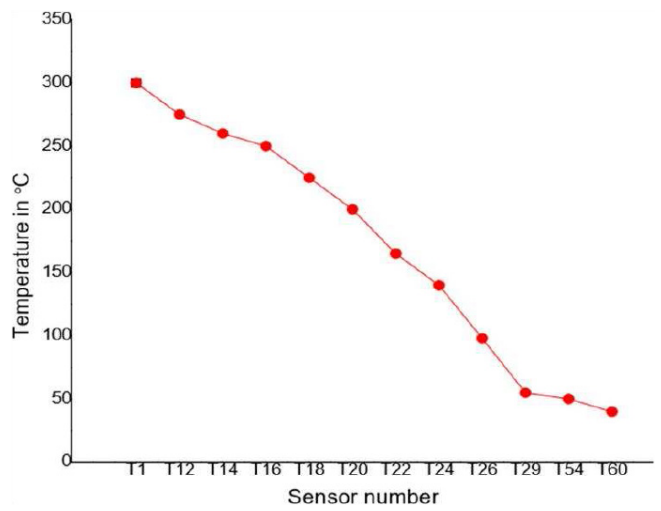


Fig. 13. Temperature distribution when main vessel is set at 300°C.

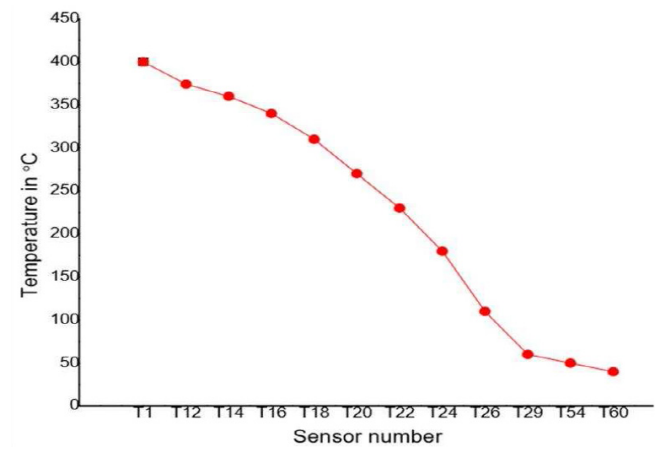


Fig. 14. Temperature distribution when main vessel is set at 400°C.

12. Experimental results vs. numerical results

Figs. 17–22 show the numerical analysis: the temperature of main vessel (heater plate) sets at different temperature level of 100°C, 200°C, 300°C, 400°C, 500°C and 577°C; and the temperature at various locations of the model are analyzed in the reactor vault.

13. Validation of experimental results with numerical analysis

Figs. 23–28 show the comparison of temperature distribution obtained by experimental and numerical values. — The temperature values obtained by numerical analysis. As

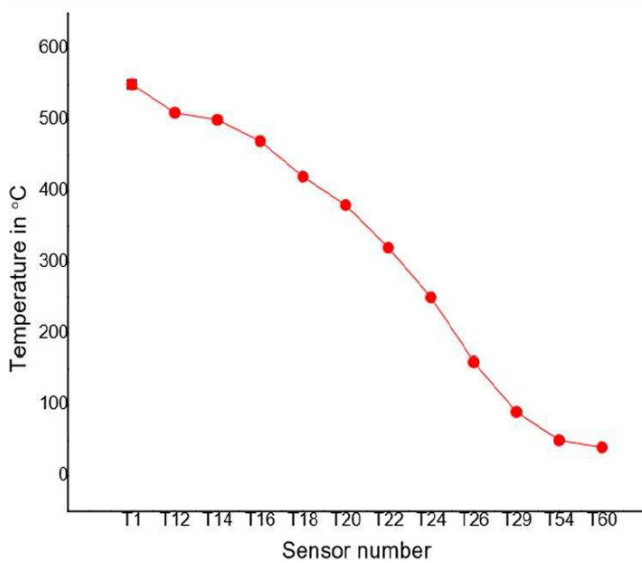


Fig. 15. Temperature distribution when main vessel is set at 500°C.

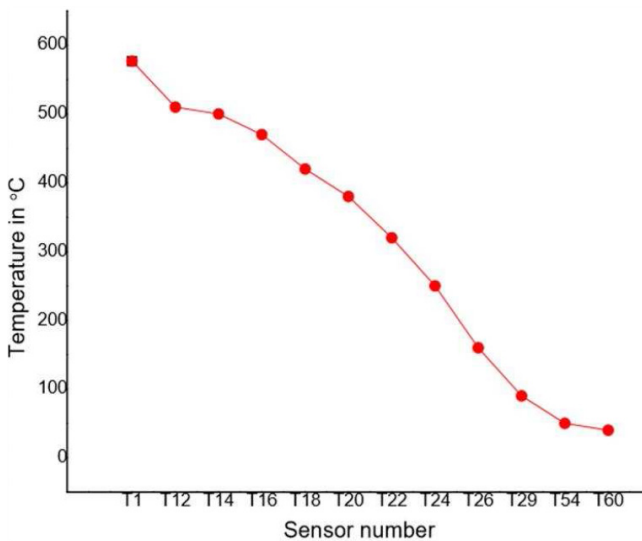


Fig. 16. Temperature distribution when main vessel is set at 577°C.

a result, it is slightly less or equal to experimental values. Therefore, the experimental results are validated by numerical analysis.

Figs. 29–34 show the temperature distribution in the cooling fluid circuit. The temperature difference between the inlet and outlet of cooling pipes are found to be 2°C–3°C.

14. Heat transfer calculations at various sections of vault

These experiments have completed with cooling circuit efficiency increased by using nanofluid. Nanoparticles have higher thermal conductivity than water molecules. The project was done by using reactor model. Experimental study is carried out on the setup by maintaining the main vessel at different temperature with all cooling pipes in open condition. The various temperature levels are measured at 64 locations in the setup with steady-state condition. The fluid circulation through the square pipes welded to liner plate is maintained at 6 lpm.

Heat transfers through the following three methods: conduction, convection and radiation. They can withstand together or individually depending on the heat source exposure and environment. The temperature within the reactor vault at certain places for finding the different temperature medium at steady-state condition. On the other hand, convection transfers the heat from the source to the main vessel to safety vessel via cycles of heating and cooling of the surrounding fluids. Radiation is the transfer of heat by electromagnetic waves. The basic one-dimensional steady

Table 1
Properties of materials

Materials	Conductivity (W/mm C)	Specific heat (J/kg C)	Density (kg/mm ³)
SS 304 L plate	0.00006	490	8.03E–6
Argon	0.0000162	523	1.661E–9
Concrete	0.0008	420	2.4E–6
EPS	3.3E–5	1.3	1E–6
MS plate	0.00006	510	8.03E–6

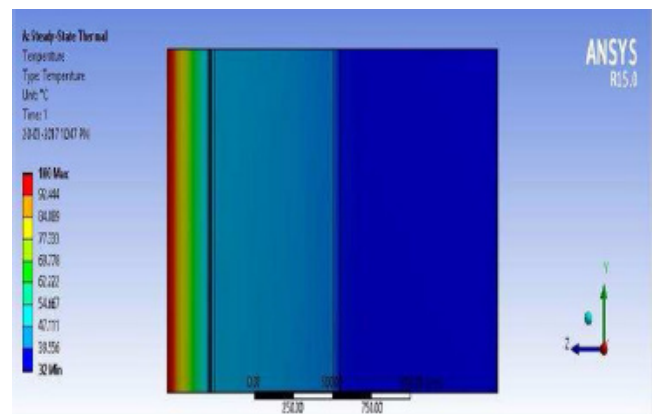


Fig. 17. The temperature distribution when main vessel is set at 100°C.

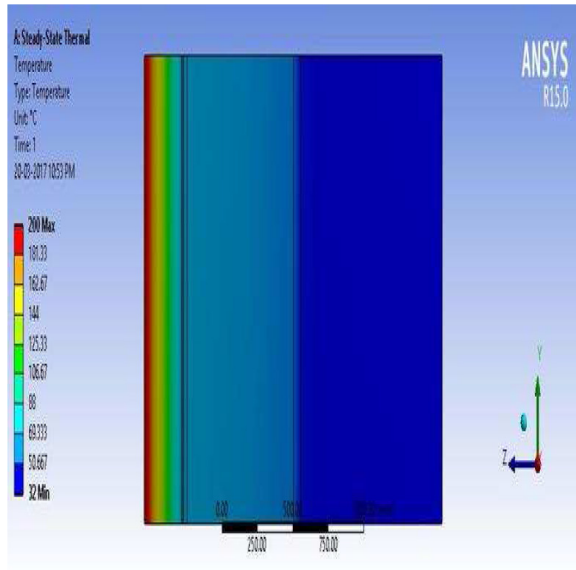


Fig. 18. The temperature distribution when main vessel is set at 200°C.

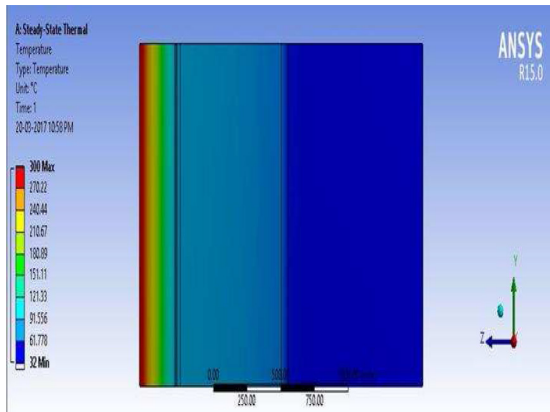


Fig. 19. The temperature distribution when main vessel is set at 300°C.

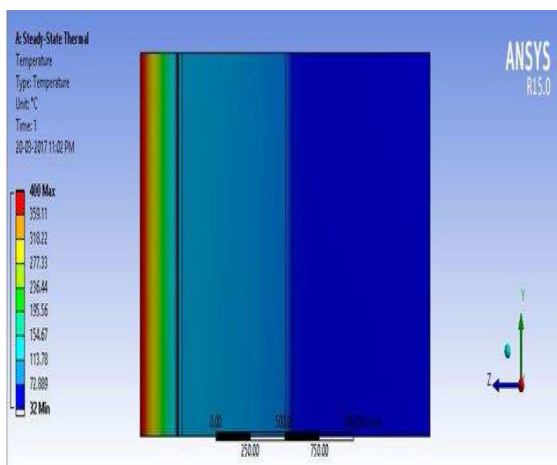


Fig. 20. The temperature distribution when main vessel is set at 400°C.

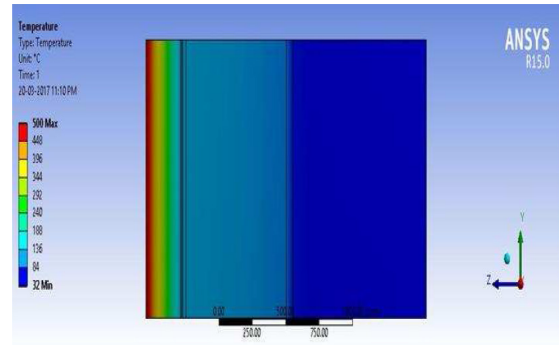


Fig. 21. The temperature distribution when main vessel is set at 500°C.

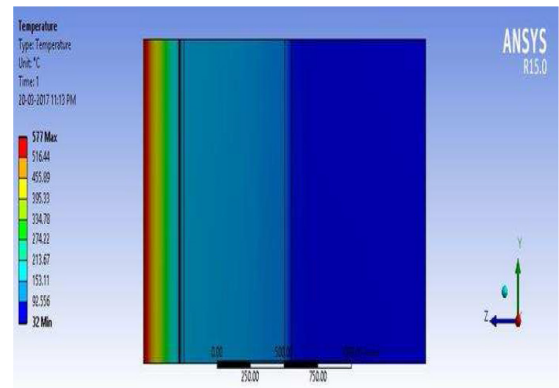


Fig. 22. The temperature distribution when main vessel is set at 577°C.

state governing equations for conduction, convection and radiation are presented in Eqs. (1) to (3), respectively.

$$q_{k_{i+0.1}} = k(dT_{i+0.1}/dx) \tag{1}$$

$$q_{h_{i+0.1}} = h\Delta T_{i+0.1} \tag{2}$$

$$q_{r_{i+0.1}} = \Phi \epsilon \sigma T_{i+0.1}^4 \tag{3}$$

q''_k is the heat flux due to conduction; q''_h is the heat flux due to convection; q_r is the heat flux due to radiation is the density; c is the specific heat; k is the conductivity; h is the convective heat transfer coefficient in $W/m^2 K$, typical value is $25 W/m^2 K$; ΔT is the temperature difference between the solid surface and fluid in ($^{\circ}C$ or K); Φ is a configuration or view factor depends on the area (A) of the emitting surface and distance (r) to the receiving surface ($\Phi = A/\pi r^2$); ϵ_i is the emissivity factor, ranging from 0 to 1.0; σ is the Stefan–Boltzmann constant taken as $(5.67 \times 10^{-8} W/m^2 K^4)$; T_e is the absolute temperature of the emitting surface (K).

15. Conclusion

Experimental study is carried out on the setup by maintaining the main vessel at different temperatures with all the cooling pipes in open condition. From the experimental

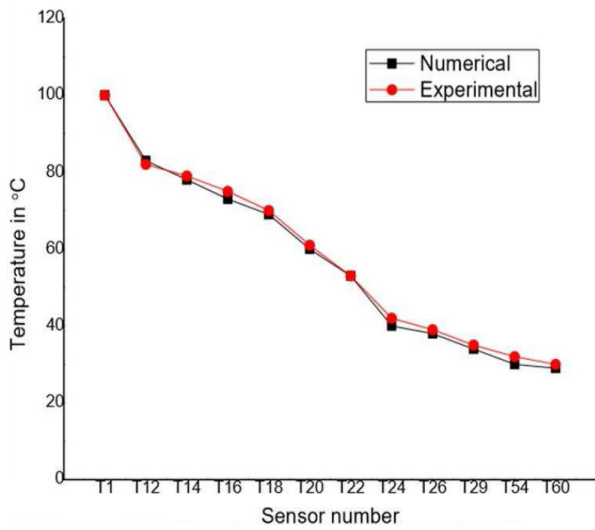


Fig. 23. Comparison of experimental value and numerical value when main vessel is set at 100°C.

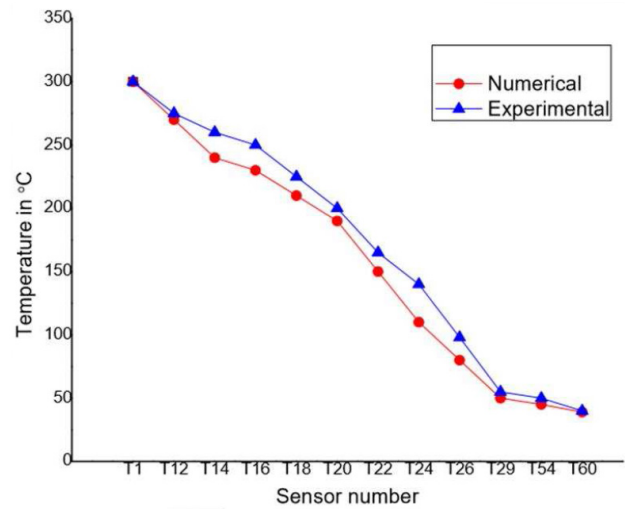


Fig. 25. Comparison of experimental value and numerical value when main vessel is set at 300°C.

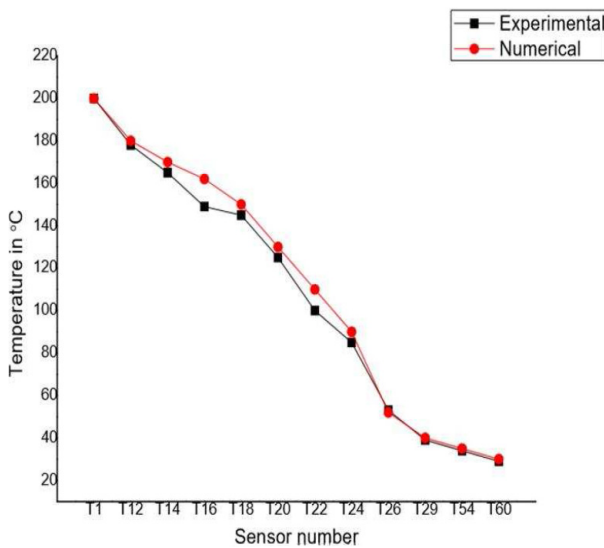


Fig. 24. Comparison of experimental value and numerical value when main vessel is set at 200°C.

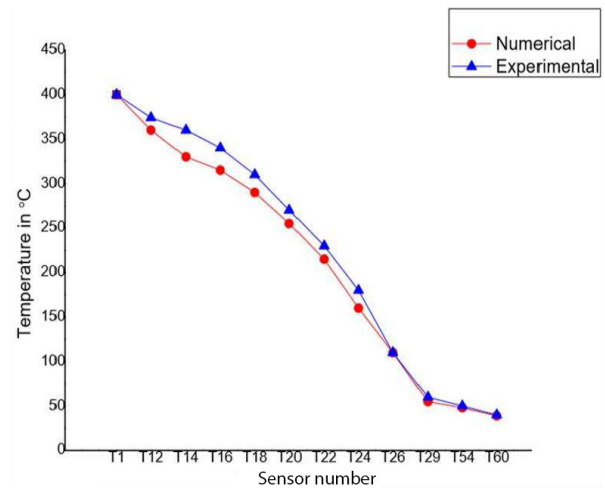


Fig. 26. Comparison of experimental value and numerical value when main vessel is set at 400°C.

study, the following conclusions have been drawn. When the temperature of main vessel (heater plate) is set at 100°C, the temperature difference at inner (T49) and outer faces (T55) of the inner concrete vault is 3°C, which is less than acceptable temperature difference. At 200°C, the temperature difference at inner (T49) and outer faces (T55) of the inner concrete vault is 5°C, which is less than acceptable temperature difference. At 300°C, the temperature difference at inner (T49) and outer faces (T55) of the inner concrete vault is 7°C, which is less than acceptable temperature difference. At 400°C, the temperature difference at inner (T49) and outer faces (T55) of the inner concrete vault is 13°C, which is less than acceptable temperature difference. At 500°C, the temperature difference at inner (T49) and outer faces (T55) of the inner concrete vault is 21°C, which is less than acceptable temperature difference.

At 577°C, the temperature difference at inner (T49) and outer faces (T55) of the inner concrete vault is 23°C, which is less than acceptable temperature difference.

When heat is transferred from inner concrete vault to outer concrete vault, there is a large temperature difference taking place between the inner concrete vault and outer concrete vault (between T55 and at T60) due to the presence of EPS sheet where the conductivity is less. Hence, the temperature at the outer face of the outer vault is maintained slightly above the room temperature in all cases.

Numerical analysis on the model is carried out using ANSYS R15.0 and the experimental results have been compared with numerical results. The temperatures obtained by numerical analysis were found to be slightly less or equal to experimental temperature values when the main vessel was set at different temperatures. Therefore, the experimental results were validated by numerical analysis.

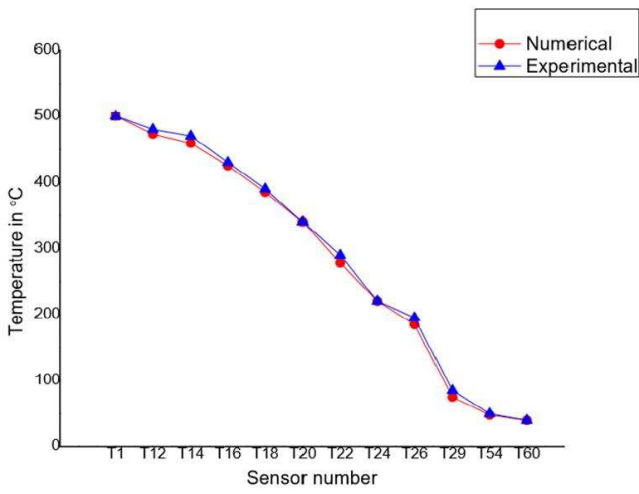


Fig. 27. Comparison of experimental value and numerical value when main vessel is set at 500°C.

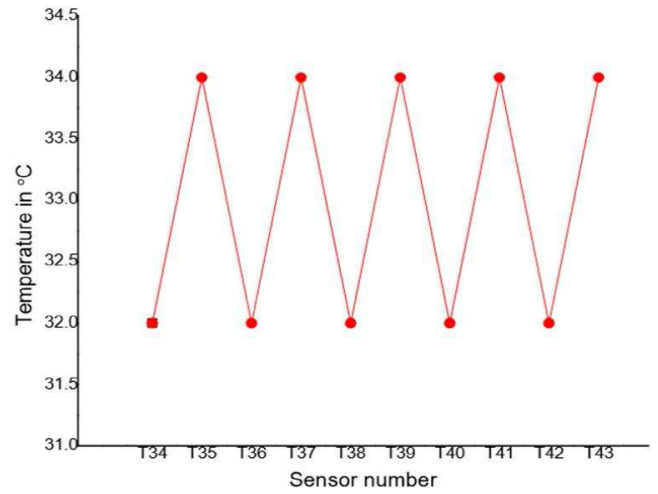


Fig. 30. Temperature distribution of cooling fluid circuit at 200°C.

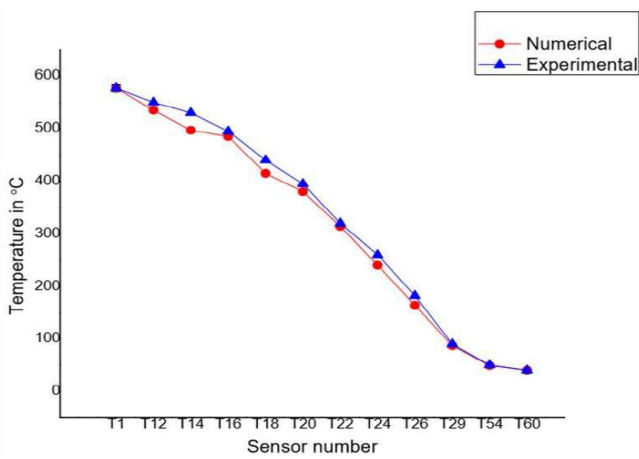


Fig. 28. Comparison of experimental value and numerical value when main vessel is set at 577°C.

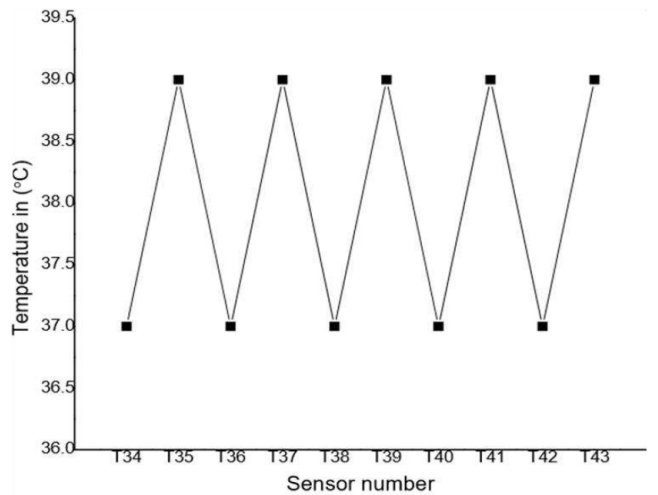


Fig. 31. Temperature distribution of cooling fluid circuit at 300°C.

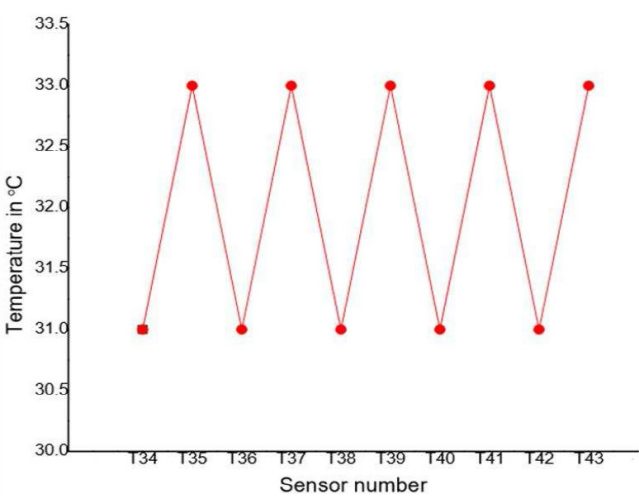


Fig. 29. Temperature distribution of cooling fluid circuit at 100°C.

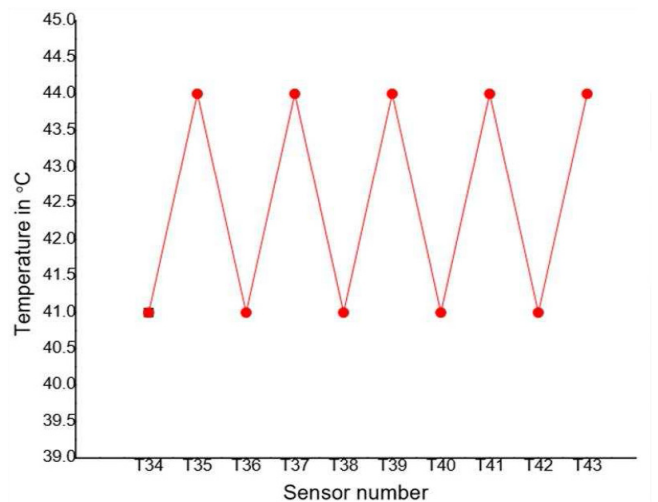


Fig. 32. Temperature distribution of cooling fluid circuit at 400°C.

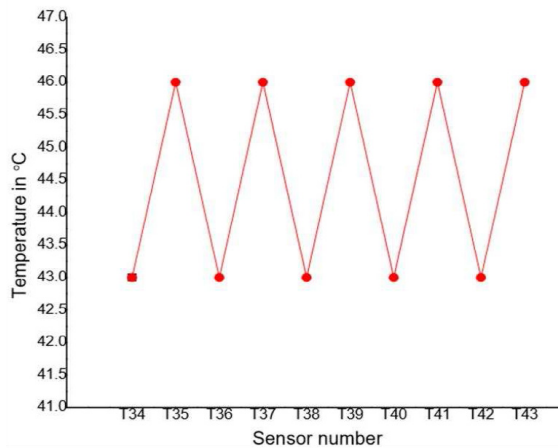


Fig. 33. Temperature distribution of cooling fluid circuit at 500°C.

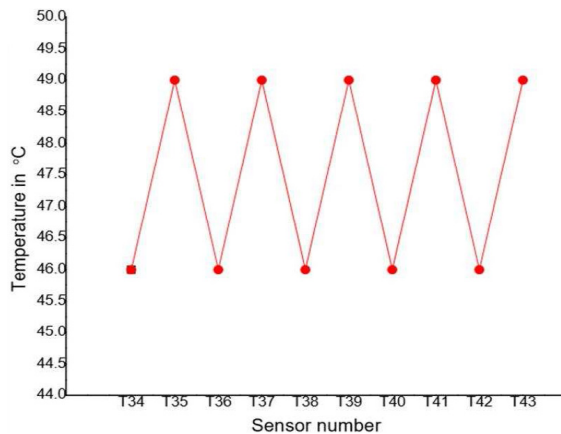


Fig. 34. Temperature distribution of cooling fluid circuit at 577°C.

Symbols

SS Grade 304	—	Stainless steel-Grade 304
SEM	—	Scanning electron microscope
EPS	—	Expanded polystyrene

Greek

Φ	—	Volumetric concentration of nanoparticles (%)
k	—	Thermal conductivity in W/m K
h	—	Heat transfer coefficient in W/m ² K
q	—	Rate of heat transfer
ϵ_i	—	Emissivity factor
T_c	—	Absolute temperature

Subscripts

e	—	Effective
r	—	Relative

References

[1] M.M. Sarafraz, F. Hormozi, Comparatively experimental study on the boiling thermal performance of metal oxide and multi-walled carbon nanotube nanofluids, *Powder Technology*, 287 (2016) 412–430.

[2] M.M. Sarafraz, Nucleate pool boiling of aqueous solution of citric acid on a smoothed horizontal cylinder, *Heat Mass Transfer*, 48 (2012) 611–619.

[3] E. Salari, S.M. Peyghambarzadeh, M.M. Sarafraz, F. Hormozi, Boiling thermal performance of TiO₂ aqueous nanofluids as a coolant on a disc copper block, *Period. Polytech. Chem. Eng.*, 60 (2016) 106–122.

[4] M.M. Sarafraz, S.M. Peyghambarzadeh, S.A. Alavifazel, Enhancement of nucleate pool boiling heat transfer to dilute binary mixtures using endothermic chemical reactions around the smoothed horizontal cylinder, *Heat Mass Transfer*, 48 (2012) 1755–1765.

[5] S.K. Das, N. Putra, W. Roetzel, Pool boiling of nanofluids on horizontal narrow tubes, *Int. J. Multiphase Flow*, 29 (2003) 1237–1247.

[6] M. Kamalgharibi, F. Hormozi, S.A.H. Zamzamin, M.M. Sarafraz, Experimental studies on the stability of CuO nanoparticles dispersed in different base fluids: influence of stirring, sonification and surface active agents, *Heat Mass Transfer*, 52 (2016) 55–62.

[7] M.M. Sarafraz, A. Arya, H. Nikkhah, On the convective thermal performance of a CPU cooler working with liquid gallium and CuO/water nanofluid: a comparative study, *Appl. Therm. Eng.*, 112 (2017) 1373–1381.

[8] F.I. El-Hosiny, N.A. El-Faramawy, Shielding of gamma radiation by hydrated Portland cement-lead pastes, *Radiat. Meas.*, 32 (2000) 93–99.

[9] A.M. El-Khayatt, Radiation shielding of concretes containing different lime/silica ratios, *Ann. Nucl. Energy*, 37 (2010), 991–995.

[10] M.H. Kharita, M. Takeyeddin, M. Alnassar, S. Yousef, Development of special radiation shielding concretes using natural local materials and evaluation of their shielding characteristics, *Progr. Nucl. Energy*, 50 (2008) 33–36.

[11] H.S. Armelin, N. Cherry, Evaluation of the use and performance of thermal radiation barriers in construction, *E-magazine Mat.*, 1 (2004) 79–82.

[12] S.M. Bajorek, J.R. Lloyd, Experimental investigation of natural convection in partitioned enclosures, *J. Heat Transfer*, 104 (2009) 527–531.

[13] M. Ciofalo, T.G. Karayiannis, Natural convection heat transfer in a partially—or completely—partitioned vertical rectangular enclosure, *Int. J. Heat Mass Transfer*, 34 (1991) 167–179.

[14] S.P. Jesumathy, M. Udayakumar, S. Suresh, Heat transfer characteristics in latent heat storage system using paraffin wax, *J. Mech. Sci. Technol.*, 26 (2012) 959–965.

[15] S. Lorente, Heat losses through building walls with closed, open and deformable cavities, *Int. J. Energy Res.*, 26 (2002) 611–632.

[16] H. Manz, Numerical simulation of heat transfer by natural convection in cavities of facade elements, *Energy Buildings*, 35 (2003) 305–311.

[17] I. Akkurt, H. Akyildirim, B. Mavi, Ş. Kilincarslan, C. Basyigit, Gamma-ray shielding properties of concrete including barite at different energies, *Progr. Nucl. Energy*, 52 (2010) 620–623.

[18] I. Akkurt, C. Basyigit, S. Kilincarslan, B. Mavi, The shielding of γ -rays by concretes produced with barite, *Progr. Nucl. Energy*, 46 (2005) 1–11.

[19] S.M. Bajorek, J.R. Lloyd, Experimental investigation of natural convection in partitioned enclosures, *J. Heat Transfer*, 104 (2008) 527–531.

[20] C. Başığit, B. Comak, S. Kilincarslan, Assessment of concrete compressive strength by image processing technique, *Construct. Build. Mater.*, 37 (2012) 526–532.

[21] C.A.N. Dare, L.A. Targa, M. Isa, Evaluating the effectiveness of thermal insulation by reflection, used as under-coverage, *Energy Agric. Botucatu*, 20 (2005) 14–29.

[22] J.G.A. De Graff, E.F.M. van der Held, The relation between the heat transfer and the convection phenomena in enclosed plane air layers, *Appl. Sci. Res.*, 3 (1952) 393–409.

[23] J.J. del Coz Díaz, P.J. Garcia Nieto, C. Betegon Biempica, M.P. Prendes Gero, Analysis and optimization of the heat-insulating light concrete hollow brick walls design by the finite element method, *Appl. Therm. Eng.*, 27 (2007) 1445–1456.

[24] W. Yu, D.M. France, E.V. Timofeeva, D. Singh, J.L. Routbort, Thermophysical property-related comparison criteria for nanofluid heat transfer enhancement in turbulent flow, *Appl. Phys.*, 96 (2010) 213109.